Available online at www.sciencedirect.com

ScienceDirect

Procedia Engineering 199 (2017) 2657–2662

Procedia Engineering

www.elsevier.com/locate/procedia

X International Conference on Structural Dynamics, EURODYN 2017

On the spectrum of rail vibration generated by a passing train

V. G. Cleante[a]*, M, J. Brennan[a], G. Gatti[b], D. J. Thompson[c]

[a]*Departamento de Engenharia Mecânica, Universidade Estadual Paulista (UNESP), Ilha Solteira, 15385-000, Sao Paulo, Brazil*
[b]*Department of Mechanical, Energy and Management Engineering, Univeristy of Calabria, Arcavacata di Rente (CS) 87036, Italy*
[c]*Institute of Sound and Vibration Research, University of Southampton, Southampton, SO17 1BJ, United Kingdom*

Abstract

Recent work in rail vibration has investigated methods for estimating track support stiffness from trackside vibration. This vibration, induced by the passage of a train, is mainly due to the load applied by the wheels, and is known as quasi-static excitation. It is characterized by dominant peaks in the vibration spectrum that are an integer multiple of the ratio between the speed and length of a train carriage. In this paper the behaviour of the vertical rail deflection is investigated to determine the physical reasons why the vibration at certain frequencies is greater than at others. A simple model is used to determine the contribution of the train geometry and the track parameters to the shape of the rail deflection spectrum. The model is also validated with data from various trains and at various sites. It is found that the track properties influence the range of frequencies at which there is significant vibrational energy, but the specific frequencies where there is large vibration are mainly a function of the train geometry.

© 2017 The Authors. Published by Elsevier Ltd.
Peer-review under responsibility of the organizing committee of EURODYN 2017.

Keywords: trackside vibration; support stiffness; trainload frequency

1. Introduction

The increase in demand for high speed trains brings some undesirable problems, such as noise and vibration [1]. Much effort has been applied to increase the performance of high-speed trains. Equally, much effort has been spent reducing vibration to improve passenger comfort and to reduce the discomfort of those who live near to railway lines.

* Corresponding author. Tel.: +55-18-37431108;
E-mail address: vinicius_cleante@hotmail.com

1877-7058 © 2017 The Authors. Published by Elsevier Ltd.
Peer-review under responsibility of the organizing committee of EURODYN 2017.
10.1016/j.proeng.2017.09.532

Trackside vibration is seen as potential energy source to power wireless sensors for structural health monitoring purposes [2,3]. However the frequency of excitation needs to be known precisely, so that tuned energy harvesting devices can be used efficiently [4]. The dominant response frequencies of the track due to the passage of a train are due to the stiffness properties of the track and the train geometry [6,7]. The aim of this paper is to further investigate the way in which these characteristics change with different sites, and to determine if there is some common behaviour that could be used in the design of an energy harvester.

2. Problem formulation

A representation of a rail track is shown in Fig. 1(a). The rail is fastened by clips to a concrete sleeper, which is supported by ballast and subgrade. This comprises the support stiffness. A schematic of the excitation mechanism for a single carriage is shown in Fig. 1(b). Moving point forces are applied to the track by each wheel. The simplified model of the complete system for a single wheel is shown in Fig. 1(c) and is discussed later.

Measured data for three different trains and from two sites are considered. One is from an Inter-city 125 with speeds of 162 and 200 km/h [5], and the other two are from a Pendolino at a speed of 195 km/h and a Supervoyager at a speed of 202 km/h [6]. In each case, vertical vibration of the sleeper is measured. Table 1 summarizes the track and train parameters.

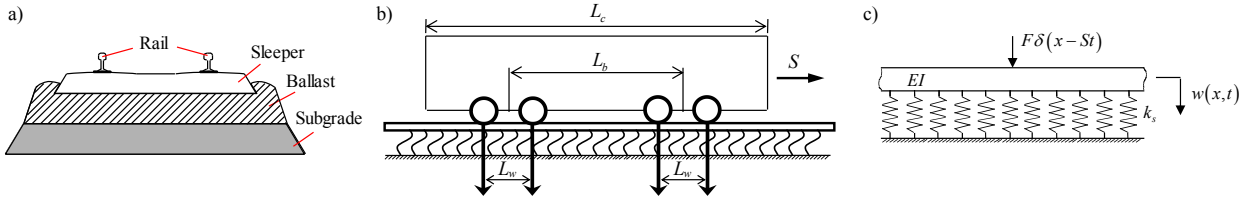

Fig. 1. (a) example of the rail track structure; (b) example of the load applied by each wheel of a carriage and (c) a simplified model of the track structure consisting of an Euler-Bernoulli infinite beam on a Winkler foundation subject to a concentrated load.

Table 1 – Characteristics of sites and train parameters [5,6].

	Track parameters			Train parameters				
Site	Rail bending stiffness [MNm^2]	Rail pad stiffness – k_p [MN/m]	Sleeper spacing [m]	Train class	Train	Carriage length [m] – L_c	Bogie length [m] – L_w	Distance between bogie centres [m] – L_b
1	EI = 6.26	k_p = 60	0.60	Mk3	Inter-city 125	23.0	2.6	16.0
2	EI = 6.26	k_p = 60	0.65	390	Pendolino	23.9	2.7	17.0
2	EI = 6.26	k_p = 60	0.65	221	Supervoyager	22.9	2.6	15.9

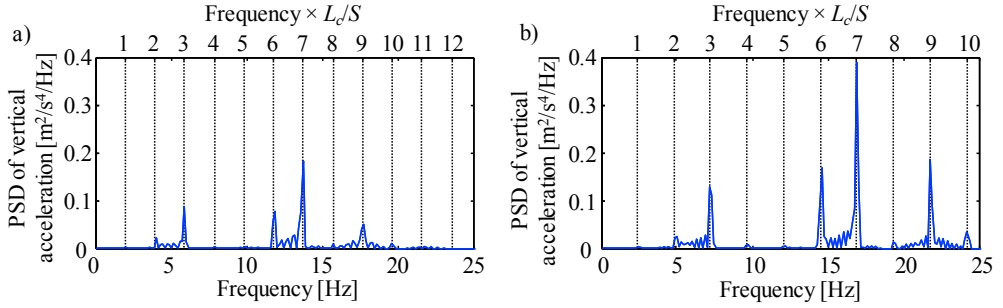

Fig. 2. PSD of sleeper vertical acceleration due to the passage of an Inter-city 125 at speeds of: a) 162 km/h; b) 200 km/h. Above the graphs, the auxiliary axis represents the frequency normalized by the ratio between the train speed and carriage length.

To illustrate typical spectra, the power spectral density (PSD) due to the passage of an Inter-city train at speeds of 162 and 200 km/h are shown in Fig. 2(a) and (b), respectively. At the top of the PSD plots another axis is shown, which represents the frequency normalized by the ratio between the train speed, S, and length of the carriage, L_c, i.e. the trainload frequency. It can be seen that the PSD is dominated by peaks that occur when the trainload frequencies are integer multiples S/L_c, which is due to the quasi-static excitation [7]. An increase (decrease) of train speed shifts the dominant peaks to higher (lower) frequencies, and changes the relative amplitudes of the dominant peaks. In Fig. 2(a) and (b), it can be seen that the 7th trainload frequency is the dominant frequency. As will be shown later, this also occurs for other trains, and the reason why this is so is examined in this paper.

3. Modelling

The model used to investigate the spectral content of the vertical track vibration is described in this section. As the frequency range of interest is less than 100 Hz [1,8–11], an Euler-Bernoulli beam on a Winkler foundation with stiffness $k_s = (L_s/k_p + 1/k_t)^{-1}/L_s$ is used, where k_p is the rail pad stiffness and k_t is the track-bed stiffness per unit length. The model is shown in Fig. 1(c) with a single moving load applied. The equation of motion for this system is given by [12]

$$EI\frac{\partial^4 w(x,t)}{\partial x^4} + k_s\, w(x,t) = F\delta(x - St) \tag{1}$$

where EI is the rail bending stiffness, $w(x,t)$ is the rail deflection, F is moving load, δ is the Dirac delta function, x is the position of each wheel in relation to the first one, and t is time. Solving Eq. (1) and noting that the relationship between sleeper and rail deflection is given by $w_s(x,t)/w(x,t) = k_s/k_t$ [1], results in [12]

$$w_s(x,t) = -\frac{F\beta}{2k_t} e^{-\beta|x-St|}\left[\cos\left(\beta|x-St|\right) + \sin\left(\beta|x-St|\right)\right] \tag{2}$$

where $\beta = (k_s/(4EI))^{1/4}$. The Eq. (2) can be written in non-dimensional form as

$$\hat{w}_s(\hat{x},\hat{t}) = \frac{w_s(x,t)}{F/(2k_t L_c)} = -\alpha e^{-\alpha|\hat{x}-\hat{t}|}\left[\cos\left(\alpha|\hat{x}-\hat{t}|\right) + \sin\left(\alpha|\hat{x}-\hat{t}|\right)\right] \tag{3a}$$

where $\alpha = \beta L_c$, $\hat{x} = x/L_c$ and $\hat{t} = t/(L_c/S)$. The normalized acceleration of the sleeper is found by differentiating Eq. (3a) twice with respect to the non-dimensional time to give

$$\ddot{\hat{w}}_s(\hat{x},\hat{t}) = 2\alpha^3 e^{-\alpha|\hat{x}-\hat{t}|}\left[\cos\left(\alpha|\hat{x}-\hat{t}|\right) - \sin\left(\alpha|\hat{x}-\hat{t}|\right)\right] \tag{3b}$$

Equation (3b) gives the equation for a single wheel. The total sleeper vibration due to a carriage can be determined by summing the contributions from four wheel-sets.

4. Comparison of model with experimental data

The deflection of the railway track is influenced by the support stiffness, i.e. the pad and track-bed stiffness. The pad parameters are relatively easy to find using the manufacturers datasheet. However, the track-bed stiffness arises from a series combination of all the elements underneath the sleeper, and due to degradation over time, ballast migration and other factors, it is not simple to estimate this parameter. Moreover, the track-bed stiffness may vary

along a railway line and may even be different from one sleeper to another. To estimate the track-bed stiffness, an optimization procedure is used, based on the model and measured data. A two-step optimization procedure is carried out to determine the track-bed stiffness and trainload from the measured vertical vibration of a sleeper. For a single carriage, the sum of the squares of the difference between Fourier coefficients of the model and the measurement data was minimised using the *Matlab* function *optimset*. First, an optimum value of β was calculated by using normalized Fourier coefficients, and then an optimum value of the trainload was calculated using a similar procedure. The results are shown in Table 2, for the 3 different trains whose data is given in Table 1.

Table 2 – Optimal parameters of the track-bed and trainload for three different trains and two different sites.

Train class	Fixed parameter		Optimized parameter			
	Pad stiffness [MN/m]	Speed [km/h]	Load W [kN]	Track-bed stiffness [MN/m^2]	Support stiffness [MN/m^2]	β
Mk3		200	21.9	16.35	14.05	0.8661
390	$k_p = 60$	195	81.8	33.24	24.44	0.9952
221		202	120.2	46.32	30.08	1.0547

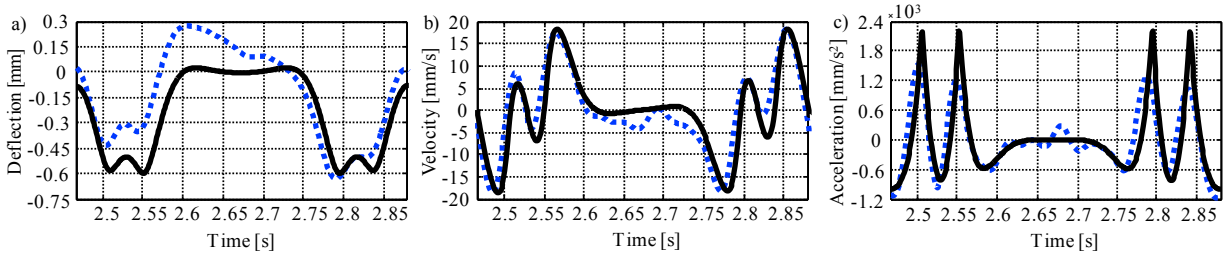

Fig. 3. Comparison of vertical vibration of the sleeper between measured data (blue dashed line, •••) and the model (black solid line, –) due to the passage of an Inter-city 125 at speed of 200 km/h: (a) displacement; (b) velocity; and (c) acceleration

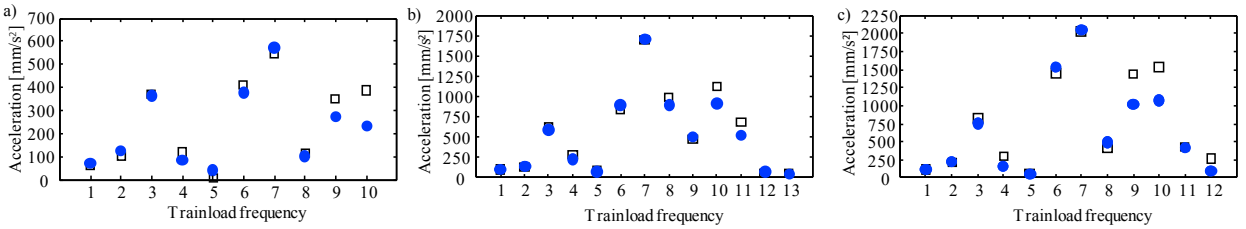

Fig. 4. Comparison between Fourier coefficients of vertical acceleration of the sleeper, measurement (blue circle, •) and model (black square, □) for: (a) Inter-city 125 at 200km/h; (b) Pendolino at 195 km/h; and (c) Supervoyager at 202 km/h.

Using the optimal parameters given in Table 2, the displacement, velocity and acceleration time-histories are plotted for an Inter-city 125 passing at speed of 200 km/h in Fig. 3. Also plotted are the measured data. It can be seen that the simple model is reasonably good at predicting the vibration of the track due to a passing train. The displacement response in Fig. 3(a), which is predicted to be predominantly below the zero-reference line, also has a response in the positive direction (in between the passing bogies) for the measured data. This is possibly due to the mass of the system, which was not accounted for in the model. Another prominent feature is that the measured acceleration does not have the sharp change in acceleration, that is evident in the predicted response. The comparison of Fourier coefficients between the vertical acceleration measured at the sleeper and the model are shown in Fig. 4. The good agreement between the model predictions and the experimental data indicates that the model captures the quasi-static vibration induced by a passing train reasonably well. It can be observed that the 3rd, 6th, 7th, 8th and 10th trainload frequencies have greater amplitudes than at the other trainload frequencies, and that the 7th trainload frequency has the largest amplitude in all cases.

5. Discussion

To determine why the amplitudes of the sleeper vibration at some trainload frequencies are greater than others and why the 7th trainload frequency has the highest amplitude of response, an investigation is carried out using the model. The effects of two fundamental parameters of the model, i.e. the support stiffness and the wheel-spacing, are considered, using the parameters of the Inter-city 125 at site 1, which are given in Tables 1 and 2, for which $\alpha = 20$. The acceleration spectrum at a measurement position for a single wheel can be determined by calculating the Fourier transform of Eq. (3b), with *x* set to zero, which result in

$$\ddot{\hat{W}} = \frac{8\alpha^4 \hat{\omega}^2}{4\alpha^4 + \hat{\omega}^4} \tag{4}$$

where $\hat{\omega} = 2\pi f \times L_i / S$ is the circular trainload frequency, in which *i* is *w* (length between bogie wheelset), or *b* (length between bogies centre), or *c* (length of the carriage). The passage of a single bogie which consists of two wheels on a rail, can be modelled using Eq. (4) and a time delay of L_w/S to give

$$\ddot{\hat{W}}\Big|_{\text{bogie}} = \frac{8\alpha^4 \hat{\omega}^2}{4\alpha^4 + \hat{\omega}^4}\left(1 + e^{-j2\pi(f \times L_w/S)}\right) \tag{5}$$

The passage of two bogies can be modelled using Eq. (5) and a time delay of L_b/S, to give

$$\ddot{\hat{W}}\Big|_{\text{two bogies}} = \ddot{\hat{W}}\Big|_{\text{bogie}}\left(1 + e^{-j2\pi(f \times L_b/S)}\right) \tag{6}$$

Equations (4), (5) and (6) are plotted in Fig. 5. Note that in Eq. (4) the acceleration is only dependent on the track. The corresponding thick solid curve in Fig. 5 describes a bandpass filter that has a peak when $\hat{\omega} = \sqrt{2}\alpha$, which is when the trainload frequency $f \times L_c / S = \alpha / \sqrt{2\pi}$. For the Inter-city 125 case considered, this is when the trainload frequency is about 4.4. This is the principal reason why the acceleration spectrum is confined to a low range of frequencies. The dashed curve depicted in Fig. 5, is the spectrum for the passing of a single bogie, given by Eq. (5). The amplitude is normalized by two, so that the shapes of the spectra can be easily compared. Note that this should be viewed with respect to the frequency axis $f \times L_w / S$. It can be seen that it is zero when $f \times L_w / S = (n + 0.5)$ for $n = 0,1,2\ldots$ The frequencies at which the amplitude is zero is only a function of the distance between the wheels on the bogie and the train speed. However, the peaks in the spectrum that occur between the zeros are dependent on both the train geometry and the track properties. The maxima of interest occur when $f \times L_w / S \approx 0.31$ and $f \times L_w / S \approx 0.83$. Thus, the bogie has created two band pass frequencies, one centred at $f \times L_c / S \approx 2.74$ and the other at $f \times L_c / S \approx 7.34$, with a zero in between these frequencies at $f \times L_c / S \approx 4.4$. Note that, in the case considered, the peak at 7.34 is larger than the peak at 2.74. The spectrum for two bogies given by Eq. (6), is also plotted in Fig. (5) as a thin solid line. Note that the amplitude is normalized by four, in this case. It can be seen that this has zeros at the same frequencies as for a single bogie, and that it has additional zeros when $f \times L_b / S = (n + 0.5)$, where $n = 0,1,2\ldots$ It also has peaks between the frequencies in between the zeros. It can be seen that the effect of the zeros is to diminish the responses at the 5th and 8th trainload frequencies.

In general, if the support stiffness is kept constant and train geometry is changed, the zeros created by the passage of one and two bogies will shift, as well as the maxima in between. However, there would have to be a considerable change (about $\pm 10\%$ of bogies centre distance) in the train geometry to cause the amplitude of another trainload frequencies, rather than the 7th, to become the largest. For the cases considered in Table 1 this is not the case. Hence, from the point of view of energy harvesting it is reasonable to target the 7th trainload frequency, independent of the type of train or the site.

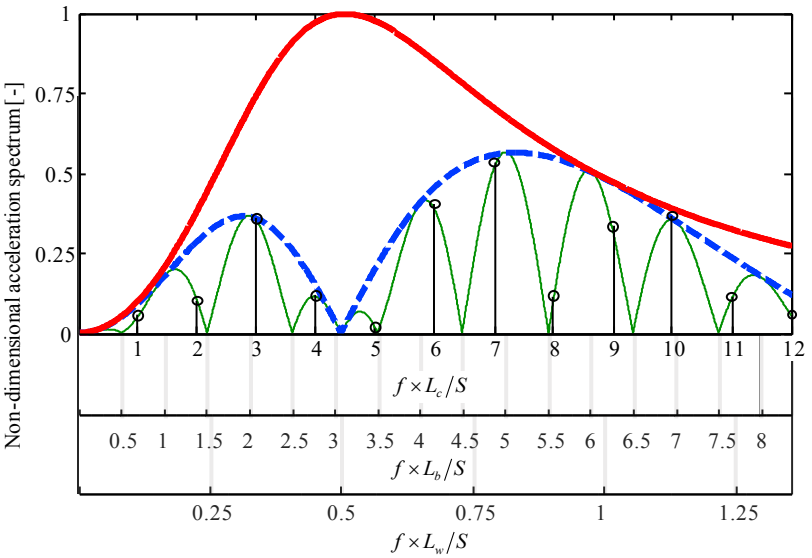

Fig. 5. Spectrum of the non-dimensional vertical acceleration of the sleeper, normalized by the maximum amplitude of one wheel spectrum. One wheel, red solid line –; one bogie, blue dashed line – –; one carriage, green thin line –; and infinite carriage, black circle ◦.

6. Conclusions

This paper has investigated the vibrational behaviour of the sleeper due to the passage of a train, and has determined the physical reasons why large vibration occurs at certain frequencies but not at others. To achieve this, a sleeper deflection model was developed and validated using experimental data from three trains at two sites.

Fourier analysis showed that the spectrum due the passage of one wheel is only dependent on the track features which acts as a bandpass filter. It is this effect that restricts to the low frequency range, the sleeper vibration due to a passing train. The train geometry, however, due to time delay from one wheel to another, has a profound effect on which specific trainload frequency has the largest response amplitude. For the trains considered, it was observed that the 3rd, 6th, 7th, 8th and 10th trainload frequencies had the highest amplitude of vibration, with the 7th trainload frequency having the highest amplitude in all cases.

References

[1] D. Thompson, Railway noise and vibration: mechanisms, modelling and means of control. Elsevier (2008).
[2] V.G. Cleante, M.J. Brennan, G. Gatti, and D.J. Thompson, Energy harvesting from the vibrations of a passing train: effect of speed variability. J. Phys.: Conf. Ser. 744 (2016) 012080.
[3] G. Gatti, M.J. Brennan, M.G. Tehrani, and D.J. Thompson, Harvesting energy from the vibration of a passing train using a single-degree-of-freedom oscillator. Mech. Sys. and Sig. Proc. 66 - 67 (2016) 785–792.
[4] C.B. Williams, C. Shearwood, M.A. Harradine, P.H. Mellor, T.S. Birch, and R.B. Yates, Development of an electromagnetic micro-generator. IEE P-Circ. Dev. Syst. 148 (2001) 337–342.
[5] N. Triepaischajonsak, The influence of various excitation mechanisms on ground vibration from trains. University of Southampton. (2012).
[6] L.L. Pen, D. Milne, D. Thompson, and W. Powrie, Evaluating railway track support stiffness from trackside measurements in the absence of wheel load data. Can. Geotech. J. 53 (2016) 1156–1166.
[7] S.-H. Ju, H.-T. Lin, and J.-Y. Huang, Dominant frequencies of train-induced vibrations. J. of Sound. and Vib. 319 (2009) 247–259.
[8] S.L. Grassie, R.W. Gregory, D. Harrison, and K.L. Johnson, The Dynamic Response of Railway Track to High Frequency Vertical Excitation. J. Mech. Eng. Scie. 24 (1982) 77–90.
[9] V. Krylov and C. Ferguson, Calculation of low-frequency ground vibrations from railway trains. Appl. Acoustics 42 (1994) 199–213.
[10] X. Sheng, C.J.C. Jones, and M. Petyt, Ground vibration generated by a load moving along a railway track. J. of Sound and Vib. 228 (1999) 129–156.
[11] X. Sheng, C.J.C. Jones, and D.J. Thompson, A theoretical study on the influence of the track on train-induced ground vibration. J. of Sound and VIb. 272 (2004) 909–936.
[12] L. Fryba, Vibration of Solids and Structures Under Moving Loads. Thomas Telford (1999).